

Quasi-particle propagation across semiconductor–Mott insulator interfaces

Jan Verlage,¹ Friedemann Queisser,^{2,3} Nikodem Szpak,¹ Jürgen König,¹ Peter Kratzer,¹ and Ralf Schützhold^{2,3}

¹*Fakultät für Physik and CENIDE, Universität Duisburg-Essen, Lotharstraße 1, 47057 Duisburg, Germany,*

²*Helmholtz-Zentrum Dresden-Rossendorf, Bautzner Landstraße 400, 01328 Dresden, Germany,*

³*Institut für Theoretische Physik, Technische Universität Dresden, 01062 Dresden, Germany,*

(Dated: May 9, 2023)

As a prototypical example for a heterostructure combining a weakly and a strongly interacting quantum many-body system, we study the interface between a semiconductor and a Mott insulator. Via the hierarchy of correlations, we derive and match the propagating or evanescent quasi-particle solutions on both sides. While the propagation is described by a band-like dispersion in both the weakly and the strongly interacting case, the inverse decay length across the interface follows a different dependence on the band gap in the Mott insulator and the semiconductor. As one consequence, tunnelling through a Mott insulating layer behaves quite different from a semiconducting (or band insulating) layer. For example, we find a strong suppression of tunnelling for energies in the middle between the upper and lower Hubbard band of the Mott insulator.

I. INTRODUCTION

The proper understanding of strongly interacting quantum many-body systems is one of the grand challenges of theoretical physics. Weakly interacting systems which can be treated via perturbation theory with respect to the small coupling strength typically display universal features. In contrast, strongly interacting systems feature new phenomena and require the development of different approaches and methods, such as strong-coupling perturbation theory [1, 2], dynamical mean-field theory [3], numerical diagonalization [4–7].

The treatment of a heterostructure combining a weakly and a strongly interacting quantum many-body system will then be even more challenging because the approach suited for describing the strongly interacting system (e.g., strong-coupling perturbation theory) may not be applicable to the weakly interacting system and vice versa. Moreover, a related situation occurs in electronic transport through a system where the electronic interaction in one subsystem is strong, e.g. through a molecular layer or quantum dots. The need to describe such systems has prompted the development of a special branch of density functional theory, the so-called i-DFT for stationary currents [8, 9]. In the present work, we employ a discrete lattice model of solids that provides a mathematical description of systems with a well-defined amount of electronic correlations. As a prototypical example for such a heterostructure, we study the interface between a semiconductor (where the interactions between the electrons can simply be included in the effective potential seen by the electrons) and a Mott insulator (where the interactions play a major role). The fabrication of these systems [10, 11] as well as the theoretical investigation how properties carry over through the interfaces [12–15] has advanced over the years.

The goal is to derive the propagating or evanescent quasi-particle modes and to match them across the interface. To this end, we employ the method of the hierarchy of correlations which is based on a formal expansion into

powers of the coordination number Z (which is assumed to be large) [16, 17]. In contrast to many other methods, this approach can be applied to the regions of weak and strong interactions on the same footing and allows us to derive the propagation of quasi-particle modes. As a major result, we give explicit expressions for the transmitted and reflected current densities as functions of energy.

II. EXTENDED FERMI-HUBBARD MODEL

In order to start with a tight-binding model which is capable of describing the relevant (valence or conduction) band of a semiconductor as well as a Mott insulator, we employ the extended Fermi-Hubbard model [18]

$$\hat{H} = -\frac{1}{Z} \sum_{\mu\nu s} T_{\mu\nu} \hat{c}_{\mu s}^\dagger \hat{c}_{\nu s} + \sum_{\mu} U_{\mu} \hat{n}_{\mu}^{\uparrow} \hat{n}_{\mu}^{\downarrow} + \sum_{\mu s} V_{\mu} \hat{n}_{\mu s}. \quad (1)$$

As usual, $\hat{c}_{\mu s}^\dagger$ and $\hat{c}_{\nu s}$ denote the fermionic creation and annihilation operators at the lattice sites μ and ν with spin $s \in \{\uparrow, \downarrow\}$ and $\hat{n}_{\mu s}$ are the associated number operators. The hopping matrix $T_{\mu\nu}$ equals the tunneling strength T for nearest neighbors μ and ν and is zero otherwise. Here we assume that the Mott insulator and the semiconductor have the same hopping strength T but our results can be generalized to different hopping strengths T for the two regions or for the different directions in a straightforward manner. The coordination number Z counts the number of nearest neighbors μ for a given lattice site ν and is assumed to be large, $Z \gg 1$. The on-site repulsion U_{μ} and potential V_{μ} are then used to distinguish the Mott insulating from the semiconducting region.

A. Hierarchy of correlations

We consider the reduced density matrices, $\hat{\rho}_{\mu}$ of one lattice site, $\hat{\rho}_{\mu\nu}$ of two, and so on. Moreover, we split

up the correlated parts via $\hat{\rho}_{\mu\nu}^{\text{corr}} = \hat{\rho}_{\mu\nu} - \hat{\rho}_\mu \hat{\rho}_\nu$, and similarly for three-site and higher-order correlations. Based on the assumption $Z \gg 1$, we may employ an expansion into powers of $1/Z$ where we find that higher-order correlators are successively suppressed. The two-point correlator scales as $\hat{\rho}_{\mu\nu}^{\text{corr}} = \mathcal{O}(1/Z)$, while the three-point correlation is suppressed as $\hat{\rho}_{\mu\nu\lambda}^{\text{corr}} = \mathcal{O}(1/Z^2)$, and so on.

Starting from the exact evolution equations ($\hbar = 1$)

$$\begin{aligned} i\partial_t \hat{\rho}_\mu &= F_1(\hat{\rho}_\mu, \hat{\rho}_{\mu\nu}^{\text{corr}}), \\ i\partial_t \hat{\rho}_{\mu\nu}^{\text{corr}} &= F_2(\hat{\rho}_\mu, \hat{\rho}_{\mu\nu}^{\text{corr}}, \hat{\rho}_{\mu\nu\lambda}^{\text{corr}}), \end{aligned} \quad (2)$$

we may now approximate them by using the expansion into powers of $1/Z$. The first evolution equation then becomes $i\partial_t \hat{\rho}_\mu = F_1(\hat{\rho}_\mu, 0) + \mathcal{O}(1/Z)$. Its zeroth-order solution $\hat{\rho}_\mu^0$ yields the mean-field background. For a more detailed view see Appendix A or [17].

In order to describe the Mott insulator, we choose

$$\hat{\rho}_\mu^0 = \frac{|\uparrow\rangle_\mu \langle \uparrow| + |\downarrow\rangle_\mu \langle \downarrow|}{2}, \quad (3)$$

while the semiconductor is represented by $\hat{\rho}_\mu^0 = |\uparrow\downarrow\rangle_\mu \langle \uparrow\downarrow|$ for the valence band and by $\hat{\rho}_\mu^0 = |0\rangle_\mu \langle 0|$ for the conduction band (at zero temperature). Note that the two cases are related to each other via particle-hole duality (such that it would be enough to consider one case only).

B. Quasi-particle operators

The propagation of quasi-particles is then governed by the linearization $i\partial_t \hat{\rho}_{\mu\nu}^{\text{corr}} \approx F_2(\hat{\rho}_\mu^0, \hat{\rho}_{\mu\nu}^{\text{corr}}, 0)$ of the second equation (2). To analyze the evolution, it is useful to introduce the quasi-particle and hole operators

$$\hat{c}_{\mu s I} = \hat{c}_{\mu s} \hat{n}_{\mu \bar{s}}^I = \begin{cases} \hat{c}_{\mu s} (1 - \hat{n}_{\mu \bar{s}}) & \text{for } I = 0 \\ \hat{c}_{\mu s} \hat{n}_{\mu \bar{s}} & \text{for } I = 1 \end{cases}, \quad (4)$$

where \bar{s} denotes the spin state opposite to s . For example $\hat{c}_{\mu \uparrow I} = |0\rangle_\mu \langle \uparrow|$ creates an empty lattice site μ for $I = 0$ while $\hat{c}_{\mu \uparrow I} = |\downarrow\rangle_\mu \langle \uparrow\downarrow|$ annihilates a doubly occupied lattice site μ for $I = 1$. Note that these operators are approximately, but not exactly equal to the quasi-particle creation and annihilation operators for holons and doublons, see, e.g. [19].

In terms of those operators, we find the following evolution equations for the correlation functions (for $\mu \neq \nu$)

$$\begin{aligned} i\partial_t \langle \hat{c}_{\mu s I}^\dagger \hat{c}_{\nu s J} \rangle^{\text{corr}} &= \frac{1}{Z} \sum_{\lambda L} T_{\mu\lambda} \langle \hat{n}_{\mu \bar{s}}^I \rangle^0 \langle \hat{c}_{\lambda s L}^\dagger \hat{c}_{\nu s J} \rangle^{\text{corr}} \\ &\quad - \frac{1}{Z} \sum_{\lambda L} T_{\nu\lambda} \langle \hat{n}_{\nu \bar{s}}^J \rangle^0 \langle \hat{c}_{\mu s I}^\dagger \hat{c}_{\lambda s L} \rangle^{\text{corr}} \\ &\quad + (U_\nu^J - U_\mu^I + V_\nu - V_\mu) \langle \hat{c}_{\mu s I}^\dagger \hat{c}_{\nu s J} \rangle^{\text{corr}} \\ &\quad + \frac{T_{\mu\nu}}{Z} (\langle \hat{n}_{\mu \bar{s}}^I \rangle^0 \langle \hat{n}_{\nu s}^1 \hat{n}_{\nu \bar{s}}^J \rangle^0 - \langle \hat{n}_{\nu \bar{s}}^J \rangle^0 \langle \hat{n}_{\mu s}^1 \hat{n}_{\mu \bar{s}}^I \rangle^0). \end{aligned} \quad (5)$$

Here we used the abbreviation $U_\mu^I = IU_\mu$, i.e., $U_\mu^I = U_\mu$ for $I = 1$ and $U_\mu^I = 0$ for $I = 0$. Quite intuitively, the

repulsion is only felt by the particle contributions $I = 1$ but not by the hole contributions $I = 0$. Expectation values denoted as $\langle \rangle^0$ are to be taken in the zeroth order solution $\hat{\rho}_\mu^0$.

The stationary source term in last line of Eq. 5 can be used to derive the ground-state correlations. However, it is not relevant for quasi-particle propagation which corresponds to solutions $\langle \hat{c}_{\mu s I}^\dagger \hat{c}_{\nu s J} \rangle^{\text{corr}}$ oscillating in time. These oscillating solutions can be derived from the first three lines (i.e., the homogeneous part) of the above equation. Moreover, we see that the propagation in different spin sectors is decoupled.

C. Factorization

As a further simplification, it can be shown that these oscillating solutions can be obtained by the following factorization ansatz

$$\langle \hat{c}_{\mu s I}^\dagger \hat{c}_{\nu s J} \rangle^{\text{corr}} = p_{\mu s I}^* p_{\nu s J}, \quad (6)$$

where the factors $p_{\nu s I}$ obey the simple equation

$$(i\partial_t - U_\mu^I - V_\mu) p_{\mu s I} = \frac{-1}{Z} \sum_{\nu J} T_{\mu\nu} \langle \hat{n}_{\mu \bar{s}}^I \rangle^0 p_{\nu s J}. \quad (7)$$

To find the quasi-particle modes, we now seek oscillating solutions with eigen-energies E , i.e., $i\partial_t \rightarrow E$.

III. MOTT-SEMICONDUCTOR INTERFACE

To simplify the analysis, we consider a planar interface which coincides with a lattice plane. Then assuming a highly symmetric lattice such as a hyper-cubic lattice, we apply a Fourier transformation of the dependence parallel to the interface which yields the parallel hopping contribution $T_{\mathbf{k}}^{\parallel}$ (for details, consult Appendix B).

For better readability, we drop the E , s , and \mathbf{k}^{\parallel} indices from now on and arrive at

$$\begin{aligned} (E - U_\mu^I - V_\mu) p_\mu^I + \langle \hat{n}_\mu^I \rangle^0 \sum_J T_{\mathbf{k}}^{\parallel} p_\mu^J = \\ -T \frac{\langle \hat{n}_\mu^I \rangle^0}{Z} \sum_J (p_{\mu-1}^J + p_{\mu+1}^J), \end{aligned} \quad (8)$$

where $\mu \in \mathbb{Z}$ now just labels the lattice sites perpendicular to the interface.

The above equations show that the particle p_μ^1 and hole p_μ^0 contributions are linearly dependent. In the semiconductor where one of the two expectation values $\langle \hat{n}_\mu^I \rangle^0$ is always zero, we find that either p_μ^0 or p_μ^1 vanishes (conduction or valence band). In the Mott insulator, on the other hand, where these expectation values read $\langle \hat{n}_\mu^I \rangle^0 = 1/2$, particle p_μ^1 and hole p_μ^0 contributions are both present.

In those regions where U_μ , V_μ , and $\langle \hat{n}_\mu^I \rangle^0$ are constant, we may solve the difference equation (8) by the following ansatz

$$p_\mu^I = \alpha^I e^{i\kappa\mu} + \beta^I e^{-i\kappa\mu}. \quad (9)$$

Insertion of this ansatz into Eq. (8) can then be used to determine the effective wavenumber κ perpendicular to the interface.

A. Semiconductor

In order to describe the semiconductor, we choose a vanishing repulsion $U_\mu = 0$ and a constant on-site potential $V_\mu = V$, which yields the effective wavenumber

$$\cos \kappa = \frac{Z}{2T} [V - E - T_{\mathbf{k}}^{\parallel}]. \quad (10)$$

Solving this equality for E reproduces the well-known dispersion relation $E = V - T_{\mathbf{k}}$. As usual, real κ describe propagating solutions while imaginary κ correspond to evanescent modes, for example in tunneling. Note that $|\kappa|$ grows for increasing V in this case, such that the probability for tunneling through a layer of finite thickness decreases.

B. Mott insulator

The Mott insulator state corresponds to a large on-site repulsion $U_\mu = U \gg T$ which we assume to be a constant. In addition, we assume a vanishing potential $V_\mu = 0$. In this case, the effective wavenumber reads

$$\cos \kappa = \frac{Z}{2T} \left[\frac{E(U - E)}{E - U/2} - T_{\mathbf{k}}^{\parallel} \right]. \quad (11)$$

In the strongly interacting regime $U \gg T$ considered here, real solutions for κ exist only for small E (lower Hubbard band) or for $E \approx U$ (upper Hubbard band). Again, this is consistent with the dispersion relation

$$E = \frac{1}{2} \left(U - T_{\mathbf{k}} \pm \sqrt{U^2 + T_{\mathbf{k}}^2} \right), \quad (12)$$

for quasi-particles and holes, respectively.

Already at this stage, we find an important qualitative difference to a semiconductor. According to Eq. (10), $|\kappa|$ grows for increasing V as $|\kappa| \sim \ln V$. In contrast, $|\kappa|$ remains finite in the strongly interacting limit $U \rightarrow \infty$ of the Mott insulator. On the other hand, $|\kappa|$ diverges for $E = U/2$, i.e., exactly in the middle between the upper and lower Hubbard bands, resulting in a strong suppression of tunneling.

C. Reflection and transmission amplitudes

Now we are in the position to study the propagation of quasi-particles across the interface. Starting from the Mott insulator region, we may employ the following ansatz

$$\begin{pmatrix} p_\mu^0 \\ p_\mu^1 \end{pmatrix} = \mathcal{N} \begin{pmatrix} E - U \\ E \end{pmatrix} [e^{i\kappa\mu} + R e^{-i\kappa\mu}], \quad (13)$$

where \mathcal{N} is a normalization constant. As expected, the hole contributions p_μ^0 dominate for the lower Hubbard band (small E) whereas the particle contributions p_μ^1 dominate for the upper Hubbard band ($E \approx U$). In the semiconductor region, on the other hand, we have exactly $p_\mu^0 = 0$ for the conduction band (where $\hat{\rho}_\mu^0 = |0\rangle_\mu \langle 0|$) or $p_\mu^1 = 0$ for the valence band (where $\hat{\rho}_\mu^0 = |\uparrow\downarrow\rangle_\mu \langle \uparrow\downarrow|$).

Matching these two contributions across the interface allows us to derive reflection and transmission amplitudes, see Appendix C. Based on Eq. (8), we obtain the reflection amplitude

$$R = -\frac{1 - \exp\{-i(\kappa_{\text{Mott}} - \kappa_{\text{semi}})\}}{1 - \exp\{i(\kappa_{\text{Mott}} + \kappa_{\text{semi}})\}}. \quad (14)$$

where κ_{semi} and κ_{Mott} are solutions of Eq. (10) and (11), respectively. Analogous to the case of impedance matching in electrodynamics, for example, we find $R = 0$ for $\kappa_{\text{Mott}} = \kappa_{\text{semi}}$. In the continuum limit of small κ , we recover the standard expression $R = (\kappa_{\text{Mott}} - \kappa_{\text{semi}})/(\kappa_{\text{Mott}} + \kappa_{\text{semi}})$ which yields perfect reflection $R \rightarrow 1$ for strong impedance mismatch $\kappa_{\text{Mott}} \gg \kappa_{\text{semi}}$ or $\kappa_{\text{Mott}} \ll \kappa_{\text{semi}}$.

In a similar way, the transmission amplitude is obtained as

$$\mathcal{T} = \mathcal{N}(2E - U)(1 + R). \quad (15)$$

The transmission probability $|\mathcal{T}|^2$ shows similar features as known from the transmission between a semiconductor and a conventional charge-transfer insulator, see e.g. [20–22]. This is shown in Fig. 1: only if the semiconductor band edge falls into the lower or upper Hubbard band, shown between gray-dotted lines in Fig. 1, appreciable transmission is found. The parameter V is used to tune the semiconductor band edge through the relevant range of energies. However, in contrast to a conventional insulator, the transmission across the interface into the Mott insulator drops exactly to zero (in the approximation used), if V falls right in between the upper and lower Hubbard band.

The method presented here can be extended to the case of a finite number of Mott-insulator layers sandwiched between two semiconductor leads. Analytical results for the transmission probability are derived in the appendix. The Mott layer acts like a potential barrier for the electrons, similar to the results known from single-particle physics. If the energy $E \geq U$, a channel for propagation of a quasi-particle through the barrier opens up, and transmission resonances are observed as function of the

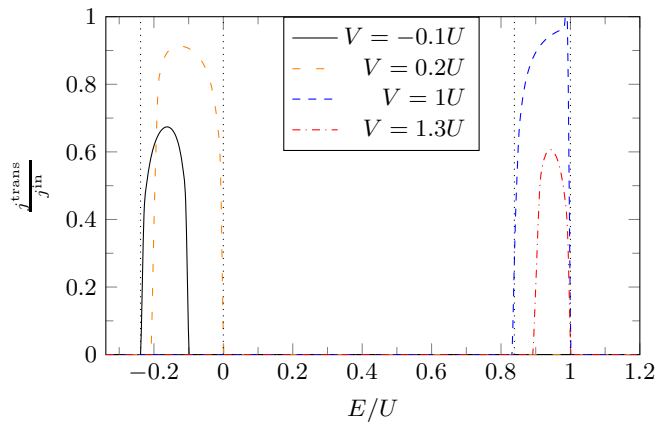


FIG. 1. (Color online) Transmission probability through the Mott insulator semiconductor interface as function of the energy E for different on-site potentials V in a two-dimensional lattice with $T_{\mathbf{k}}^{\parallel} = \frac{2T}{Z}$ and $T = 0.4U$. The gray dotted lines depict the positions of the lower (from $-0.25E/U$ to $0E/U$) and upper ($0.85E/U - 1E/U$) Hubbard band of the Mott side. The semiconductor band shifts with V .

quasi-particle energy. This is illustrated for typical parameter values in Fig. 2. For $0 < E < U$ tunneling through the barrier is observed. Again, our analytical expression shows that the tunneling probability vanishes for an energy exactly between the upper and lower Hubbard band. In App. E we present a toy model with few Mott sites between semiconducting leads to analyse and better understand the reason for this vanishing of the transmission. It is found that there is a minimum of the transmission resulting from a coherent superposition of transmission amplitudes involving the lower and the upper Hubbard band. The destructive interference of these two transmission amplitudes is responsible for the suppression of the tunneling.

IV. CONCLUSIONS

In summary, we studied the interface between a weakly interacting semiconductor and a strongly interacting Mott insulator. To this, we carried out the formal expansion into inverse powers of the coordination number $1/Z$ establishing a hierarchy of correlations. This method, in contrast to others like strong coupling perturbation theory or perturbation theory, is suited both for the strongly and weakly interacting systems. Moreover, it works for general lattices $T_{\mu\nu}$ and is particularly suited for higher dimensions. Using this method we employed the extended Fermi-Hubbard model to describe the semiconductor with a homogeneous on-site potential V and the Mott insulator with the on-site Coulomb repulsion U .

We established effective particle and hole operators $\hat{c}_{\mu s I}$ on a half-filled mean-field background and used them to calculate the time evolution of the resulting correlation

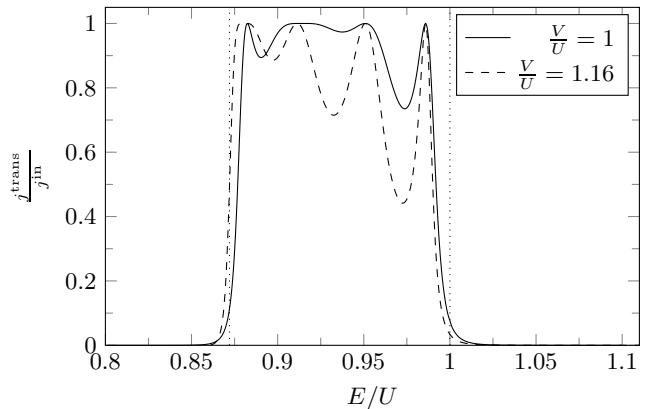


FIG. 2. Transmission through the upper Hubbard band for $T = 0.3U$ in a two-dimensional lattice with $T_{\mathbf{k}}^{\parallel} = \frac{2T}{Z}$ for two different semiconductor potentials $V = U$ and $V = 1.16U$. The dotted vertical lines mark the upper Hubbard band, and the conduction bands of the semiconductor are given approximately by the plot range. Above the Hubbard band and below, so between the two bands, there is a tunnelling current. Inside the band there are peaks to perfect transmission for energies that fulfil the resonance condition $\kappa_{\text{Mott}} \cdot \pi = zd$ with $z \in \mathbb{Z}$ with the barrier width d , they appear for all V at the same position.

functions. The homogeneous part of these equations give rise to propagating quasi-particle solutions. These solutions recover the well known dispersion relations for the semiconductor $E = V - T_{\mathbf{k}}$ as well as the two Hubbard bands at $E \approx 0$ and $E \approx U$. We calculate an analytical expression for the reflected and transmitted quasi-particle current at the interface and see that this is analogous to the case of impedance matching in electrodynamics. Lastly, already from the dispersion relation of the Mott insulator we deduct that tunneling is strongly suppressed if the energy is right in the middle between the upper and lower Hubbard bands due to destructive interference of the tunneling amplitudes from particle and hole contributions. This is confirmed by the analytical expression for the tunneling current through a semiconductor-Mott-semiconductor heterostructure.

ACKNOWLEDGMENTS

Funded by the Deutsche Forschungsgemeinschaft (DFG, German Research Foundation) – Project-ID 278162697– SFB 1242.

Appendix A: Hierarchy of correlations

As mentioned in the main text, we consider reduced density matrices $\hat{\rho}_{\mu} = \text{tr}_{\mu'}(\hat{\rho})$, $\hat{\rho}_{\mu\nu} = \text{tr}_{\mu'\nu'}(\hat{\rho})$ etc., defined by tracing out all other lattice sites. These still obey the normalization condition, e.g., $\text{tr} \hat{\rho}_{\mu} = 1$. Now, we

follow [17] by splitting up the reduced density matrices into correlated and uncorrelated parts;

$$\begin{aligned}\hat{\rho}_{\mu\nu} &= \hat{\rho}_{\mu\nu}^{\text{corr}} + \hat{\rho}_{\mu}\hat{\rho}_{\nu}, \\ \hat{\rho}_{\mu\nu\lambda} &= \hat{\rho}_{\mu\nu\lambda}^{\text{corr}} + \hat{\rho}_{\mu\nu}^{\text{corr}}\hat{\rho}_{\lambda} + \hat{\rho}_{\mu\lambda}^{\text{corr}}\hat{\rho}_{\nu} + \hat{\rho}_{\nu\lambda}^{\text{corr}}\hat{\rho}_{\mu} + \hat{\rho}_{\mu}\hat{\rho}_{\nu}\hat{\rho}_{\lambda} \\ \hat{\rho}_{\mu\nu\lambda\kappa} &= \hat{\rho}_{\mu\nu\lambda\kappa}^{\text{corr}} + \dots\end{aligned}\quad (\text{A1})$$

This is the starting point for an expansion into powers of $1/Z$ which is possible for all general lattice Hamiltonians

$$\hat{H} = \frac{1}{Z} \sum_{\mu\nu} \hat{H}_{\mu\nu} + \sum_{\mu} \hat{H}_{\mu}. \quad (\text{A2})$$

In this Hamiltonian $H_{\mu\nu}$ describes two site processes, while H_{μ} encapsulates all one site parts like a chemical potential or Coulomb repulsion. This includes both fermionic and bosonic systems. The time-evolution of a density operator is given by the von-Neumann equation ($\hbar = 1$)

$$\begin{aligned}i\partial_t \hat{\rho} &= [\hat{H}, \hat{\rho}] = \frac{1}{Z} \sum_{\mu\nu} [\hat{H}_{\mu\nu}, \hat{\rho}] + \sum_{\mu} [\hat{H}_{\mu}, \hat{\rho}] \\ &= \frac{1}{Z} \sum_{\mu\nu} \hat{\mathcal{L}}_{\mu\nu} \hat{\rho} + \sum_{\mu} \hat{\mathcal{L}}_{\mu} \hat{\rho}\end{aligned}\quad (\text{A3})$$

where we introduced the super-operators $\hat{\mathcal{L}}_{\mu\nu} = [\hat{H}_{\mu\nu}, \hat{\rho}]$ and $\hat{\mathcal{L}}_{\mu} = [\hat{H}_{\mu}, \hat{\rho}]$. Inserting Eq. A1 gives the evolution equations

$$i\partial_t \hat{\rho}_{\mu} = \frac{1}{Z} \sum_{\alpha \neq \mu} \text{tr}_{\alpha} \left(\hat{\mathcal{L}}_{\alpha\mu}^S [\hat{\rho}_{\mu\alpha}^{\text{corr}} + \hat{\rho}_{\alpha}\hat{\rho}_{\mu}] \right) + \hat{\mathcal{L}}_{\mu} \hat{\rho}_{\mu} \quad (\text{A4})$$

with the symmetrized $\hat{\mathcal{L}}_{\mu\nu}^S = \hat{\mathcal{L}}_{\mu\nu} + \hat{\mathcal{L}}_{\nu\mu}$ and

$$\begin{aligned}i\partial_t \hat{\rho}_{\mu\nu} &= \frac{1}{Z} \sum_{\alpha \neq \mu\nu} \text{tr}_{\alpha} \left(\hat{\mathcal{L}}_{\alpha\mu}^S \hat{\rho}_{\mu\nu\alpha} + \hat{\mathcal{L}}_{\nu\alpha}^S \hat{\rho}_{\mu\nu\alpha} \right) \\ &\quad + \frac{1}{Z} \hat{\mathcal{L}}_{\mu\nu} \hat{\rho}_{\mu\nu} + \hat{\mathcal{L}}_{\mu} \hat{\rho}_{\mu\nu} + \hat{\mathcal{L}}_{\nu} \hat{\rho}_{\mu\nu}.\end{aligned}\quad (\text{A5})$$

The previous equations yield the time-evolution for the two-site correlations

$$\begin{aligned}i\partial_t \hat{\rho}_{\mu\nu}^{\text{corr}} &= \hat{\mathcal{L}}_{\mu} \hat{\rho}_{\mu\nu}^{\text{corr}} + \frac{1}{Z} \hat{\mathcal{L}}_{\mu\nu} (\hat{\rho}_{\mu\nu}^{\text{corr}} + \hat{\rho}_{\mu}\hat{\rho}_{\nu}) \\ &\quad - \frac{\hat{\rho}_{\mu}}{Z} \text{tr}_{\mu} \left(\hat{\mathcal{L}}_{\mu\nu}^S [\hat{\rho}_{\mu\nu}^{\text{corr}} + \hat{\rho}_{\mu}\hat{\rho}_{\nu}] \right) \\ &\quad + \frac{1}{Z} \sum_{\alpha \neq \mu\nu} \text{tr}_{\alpha} \left(\hat{\mathcal{L}}_{\mu\alpha}^S [\hat{\rho}_{\mu\nu\alpha}^{\text{corr}} + \hat{\rho}_{\mu\nu}^{\text{corr}}\hat{\rho}_{\alpha} + \hat{\rho}_{\nu\alpha}^{\text{corr}}\hat{\rho}_{\mu}] \right) \\ &\quad + (\mu \leftrightarrow \nu).\end{aligned}\quad (\text{A6})$$

$$\begin{aligned}i\partial_t \hat{\rho}_{\mu\nu}^{\text{corr}} &= \hat{\mathcal{L}}_{\mu} \hat{\rho}_{\mu\nu}^{\text{corr}} + \frac{1}{Z} \hat{\mathcal{L}}_{\mu\nu} (\hat{\rho}_{\mu\nu}^{\text{corr}} + \hat{\rho}_{\mu}\hat{\rho}_{\nu}) \\ &\quad - \frac{\hat{\rho}_{\mu}}{Z} \text{tr}_{\mu} \left(\hat{\mathcal{L}}_{\mu\nu}^S [\hat{\rho}_{\mu\nu}^{\text{corr}} + \hat{\rho}_{\mu}\hat{\rho}_{\nu}] \right) \\ &\quad + \frac{1}{Z} \sum_{\alpha \neq \mu\nu} \text{tr}_{\alpha} \left(\hat{\mathcal{L}}_{\mu\alpha}^S [\hat{\rho}_{\mu\nu\alpha}^{\text{corr}} + \hat{\rho}_{\mu\nu}^{\text{corr}}\hat{\rho}_{\alpha} + \hat{\rho}_{\nu\alpha}^{\text{corr}}\hat{\rho}_{\mu}] \right) \\ &\quad + (\mu \leftrightarrow \nu).\end{aligned}\quad (\text{A7})$$

We see that there is a hierarchy of equations

$$\begin{aligned}i\partial_t \hat{\rho}_{\mu} &= F_1(\hat{\rho}_{\mu}, \hat{\rho}_{\mu\nu}^{\text{corr}}), \\ i\partial_t \hat{\rho}_{\mu\nu}^{\text{corr}} &= F_2(\hat{\rho}_{\mu}, \hat{\rho}_{\mu\nu}^{\text{corr}}, \hat{\rho}_{\mu\nu\lambda}^{\text{corr}}), \\ i\partial_t \hat{\rho}_{\mu\nu\lambda}^{\text{corr}} &= F_3(\hat{\rho}_{\mu}, \hat{\rho}_{\mu\nu}^{\text{corr}}, \hat{\rho}_{\mu\nu\lambda}^{\text{corr}}, \hat{\rho}_{\mu\nu\lambda\kappa}^{\text{corr}})\end{aligned}\quad (\text{A8})$$

and so on. In the limit $Z \gg 1$ higher-order correlators are successively suppressed. With this, we find a self-consistent equation for the on-site density matrix

$$i\partial_t \hat{\rho}_{\mu} = \frac{1}{Z} \sum_{\alpha \neq \mu} \text{tr}_{\alpha} \left(\hat{\mathcal{L}}_{\mu\alpha}^S \hat{\rho}_{\mu}\hat{\rho}_{\alpha} \right) + \hat{\mathcal{L}}_{\mu} \hat{\rho}_{\mu} + \mathcal{O}(1/Z). \quad (\text{A9})$$

This has a solution $\hat{\rho}_{\mu}^0$ that is needed for the two-site correlations

$$\begin{aligned}i\partial_t \hat{\rho}_{\mu\nu}^{\text{corr}} &= \hat{\mathcal{L}}_{\mu} \hat{\rho}_{\mu\nu}^{\text{corr}} + \frac{1}{Z} \hat{\mathcal{L}}_{\mu\nu} \hat{\rho}_{\mu}^0 \hat{\rho}_{\nu}^0 - \frac{\hat{\rho}_{\mu}^0}{Z} \text{tr}_{\mu} \left(\hat{\mathcal{L}}_{\mu\nu}^S \hat{\rho}_{\mu}^0 \hat{\rho}_{\nu}^0 \right) \\ &\quad + \frac{1}{Z} \sum_{\alpha \neq \mu\nu} \text{tr}_{\alpha} \left(\hat{\mathcal{L}}_{\mu\alpha}^S [\hat{\rho}_{\mu\nu}^{\text{corr}} \hat{\rho}_{\alpha}^0 + \hat{\rho}_{\nu\alpha}^{\text{corr}} \hat{\rho}_{\mu}^0] \right) \\ &\quad + (\mu \leftrightarrow \nu) + \mathcal{O}(1/Z^2).\end{aligned}\quad (\text{A10})$$

In the end, the whole hierarchy is given by

$$\begin{aligned}\hat{\rho}_{\mu} &= \mathcal{O}(Z^0), \quad \hat{\rho}_{\mu\nu}^{\text{corr}} = \mathcal{O}(1/Z), \\ \hat{\rho}_{\mu\nu\kappa}^{\text{corr}} &= \mathcal{O}(1/Z^2), \quad \hat{\rho}_{\mu\nu\kappa\lambda}^{\text{corr}} = \mathcal{O}(1/Z^3).\end{aligned}\quad (\text{A11})$$

Appendix B: Hierarchy for the extended Hubbard model

The exact time-evolution of the effective particle and hole operators defined in the main text $\hat{c}_{\mu s I}$ is given by the von-Neumann equation

$$\begin{aligned}i\partial_t \hat{c}_{\mu s I} &= \frac{-1}{Z} \sum_{\kappa \neq \mu} T_{\mu\kappa} \hat{c}_{\kappa s I} + (V_{\mu} + U_{\mu}^I) \hat{c}_{\mu s I} \\ &\quad - \frac{1}{Z} \sum_{\kappa \neq \mu} T_{\mu\kappa} \left(\hat{c}_{\kappa \bar{s}}^{\dagger} c_{\mu \bar{s}} c_{\mu s} - c_{\mu s} c_{\mu \bar{s}}^{\dagger} c_{\kappa \bar{s}} \right).\end{aligned}\quad (\text{B1})$$

Combining these and truncating after the first order in $1/Z$ we find, as in the main text,

$$\begin{aligned}i\partial_t \langle \hat{c}_{\mu s I}^{\dagger} \hat{c}_{\nu s J} \rangle^{\text{corr}} &= \frac{1}{Z} \sum_{\lambda L} T_{\mu\lambda} \langle \hat{n}_{\mu \bar{s}}^I \rangle^0 \langle \hat{c}_{\lambda s L}^{\dagger} \hat{c}_{\nu s J} \rangle^{\text{corr}} \\ &\quad - \frac{1}{Z} \sum_{\lambda L} T_{\nu\lambda} \langle \hat{n}_{\nu \bar{s}}^J \rangle^0 \langle \hat{c}_{\mu s I}^{\dagger} \hat{c}_{\lambda s L} \rangle^{\text{corr}} \\ &\quad + (U_{\nu}^J - U_{\mu}^I + V_{\nu} - V_{\mu}) \langle \hat{c}_{\mu s I}^{\dagger} \hat{c}_{\nu s J} \rangle^{\text{corr}} \\ &\quad + \frac{T_{\mu\nu}}{Z} \left(\langle \hat{n}_{\mu \bar{s}}^I \rangle^0 \langle \hat{n}_{\nu s}^1 \hat{n}_{\nu \bar{s}}^J \rangle^0 - \langle \hat{n}_{\nu \bar{s}}^J \rangle^0 \langle \hat{n}_{\mu s}^1 \hat{n}_{\mu \bar{s}}^I \rangle^0 \right)\end{aligned}\quad (\text{B2})$$

The homogeneous part, i.e. the first three lines of (B2), can be solved by the factorization *ansatz*. Moreover, for further simplification we employ a Fourier transformation parallel to the interface

$$p_{\mu s I} = \frac{1}{\sqrt{N_{\parallel}}} \sum_{\mathbf{k}_{\parallel}} p_{n, \mathbf{k}_{\parallel}, s I} e^{i \mathbf{k}_{\parallel} \cdot \mathbf{x}_{\mu}^{\parallel}} \quad (\text{B3})$$

$$T_{\mu \nu} = \frac{Z}{N_{\parallel}} \sum_{\mathbf{k}_{\parallel}} T_{m, n, \mathbf{k}_{\parallel}} e^{i \mathbf{k}_{\parallel} \cdot (\mathbf{x}_{\mu}^{\parallel} - \mathbf{x}_{\nu}^{\parallel})}. \quad (\text{B4})$$

From now on, we drop some indices $p_{n, \mathbf{k}_{\parallel}, s I} \equiv p_{\mu}^I$. As an example, the Fourier transform of the hopping matrix for nearest neighbour hopping is given by

$$T_{m, n, \mathbf{k}_{\parallel}} = \frac{T_{n, \mathbf{k}_{\parallel}}^{\parallel}}{Z} \delta_{m, n} + \frac{1}{Z} (T_{n, n-1}^{\perp} \delta_{n, n-1} + T_{n, n+1}^{\perp} \delta_{n, n+1})$$

$$T_{n, \mathbf{k}_{\parallel}}^{\parallel} = 2T_n^{\parallel} \sum_{x_i} \cos(p_{x_i}^{\parallel}) \equiv Z T_{\mathbf{k}}^{\parallel}. \quad (\text{B5})$$

In the main text, green this expression has been further simplified by assuming an isotropic hopping rate $T_n^{\parallel} = T_{n, n-1}^{\perp} = T$. The resulting effective coupled evolution equations are

$$(E - U_{\mu}^I - V_{\mu}) p_{\mu}^I + \langle \hat{n}_{\mu}^I \rangle^0 \sum_J T_{\mathbf{k}}^{\parallel} p_{\mu}^J =$$

$$-T \frac{\langle \hat{n}_{\mu}^I \rangle^0}{Z} \sum_J (p_{\mu-1}^J + p_{\mu+1}^J). \quad (\text{B6})$$

1. Semiconductor

The semiconductor has zero Coulomb repulsion $U = 0$ and a constant on-site potential $V_{\mu} = V$. $\hat{\rho}_{\mu}^0 = |\uparrow\downarrow\rangle_{\mu} \langle \uparrow\downarrow|$ describes the valence band and $\hat{\rho}_{\mu}^0 = |0\rangle_{\mu} \langle 0|$ the conduction band (at zero temperature). Consequently, either one of $\langle \hat{n}_{\mu}^I \rangle^0$ is zero. This yields a simple

$$(E - V) p_{\mu}^I + T_{\mathbf{k}}^{\parallel} p_{\mu}^J = \frac{-T}{Z} (p_{\mu-1}^I + p_{\mu+1}^I). \quad (\text{B7})$$

A propagating wave *ansatz* $e^{i \kappa \mu}$ yields the well known dispersion relation $E = V - T_{\mathbf{k}}^{\parallel} - \frac{2T}{Z} \cos \kappa = V - T_{\mathbf{k}}$. Real solutions exist for $E \in [V - T_{\mathbf{k}}^{\parallel} - \frac{2T}{Z}, V - T_{\mathbf{k}}^{\parallel} + \frac{2T}{Z}]$.

2. Mott insulator

In the Mott insulator at half filling

$$\hat{\rho}_{\mu}^0 = \frac{|\uparrow\rangle_{\mu} \langle \uparrow| + |\downarrow\rangle_{\mu} \langle \downarrow|}{2}, \quad (\text{B8})$$

the upper and lower Hubbard band solutions are related via $(E - U) p_{\mu}^1 = E p_{\mu}^0$. The plane wave *ansatz* results in

$$\cos \kappa = \frac{Z}{2T} \left[\frac{E(U - E)}{E - U/2} - T_{\mathbf{k}}^{\parallel} \right]. \quad (\text{B9})$$

that yields the well known dispersion relation of the Hubbard model. Real solutions for κ exist for $E \in [E^1, E^3]$ and $E \in [E^2, E^4]$ with

$$E^{1,2} = \frac{1}{2} \left(\frac{-2T}{Z} + T_{\mathbf{k}}^{\parallel} + U \pm \sqrt{\left(\frac{-2T}{Z} + T_{\mathbf{k}}^{\parallel} \right)^2 + U^2} \right)$$

$$E^{3,4} = \frac{1}{2} \left(\frac{2T}{Z} + T_{\mathbf{k}}^{\parallel} + U \pm \sqrt{\left(\frac{2T}{Z} + T_{\mathbf{k}}^{\parallel} \right)^2 + U^2} \right). \quad (\text{B10})$$

In the case of strong repulsion $U \gg T$ the minus or plus sign in front of the root yields the band around $E \approx 0$ and $E \approx U$, respectively.

Appendix C: Reflection and transmission amplitudes

In the following, we want to calculate the reflection and transmission amplitudes of the effective particle and hole solutions through the interface. Starting in the Mott, we employ the following ansatz

$$\begin{pmatrix} p_{\mu}^0 \\ p_{\mu}^1 \end{pmatrix} = \mathcal{N} \begin{pmatrix} E - U \\ E \end{pmatrix} [e^{i \kappa \mu} + R e^{-i \kappa \mu}] \quad (\text{C1})$$

and in the semiconductor we have

$$\begin{pmatrix} p_{\mu}^0 \\ p_{\mu}^1 \end{pmatrix} = \mathcal{M} \begin{pmatrix} x \\ 1 - x \end{pmatrix} \mathcal{T} e^{i \kappa \mu} \quad (\text{C2})$$

with normalization constants \mathcal{N} and \mathcal{M} , the reflection amplitude R and transmission amplitude \mathcal{T} . In the semiconductor $x = 1$ yields the conduction band while $x = 0$ the valance band, so $x = \langle \hat{n}_{\mu}^0 \rangle$. Due to the doublon-holon symmetry in the semiconductor we just need to calculate the reflection for one of these cases, so in the following $x = 0$. To make sense of the transmission amplitude, we need to define a probability current

$$\partial_t |p_{\mu}^0 + p_{\mu}^1|^2 + j_{\mu} - j_{\mu-1} = iU [p_{\mu}^0 (p_{\mu}^1)^* - p_{\mu}^1 (p_{\mu}^0)^*] \quad (\text{C3})$$

with

$$j_{\mu} = i \frac{T}{Z} (p_{\mu}^0 + p_{\mu}^1) (p_{\mu+1}^0 + p_{\mu+1}^1)^* + c.c. \quad (\text{C4})$$

For a single mode, like done here, the ratio p^1/p^0 equals a real value, so the right side of Eq. (C3) is zero. This permits the interpretation of j_{μ} as a probability current. From the evolution equation (B6) we deduct two boundary conditions, using $\mu < 0$ as the Mott insulator and $\mu \geq 0$ as the semiconductor

$$(E - V + T_{\mathbf{k}}^{\parallel}) p_0^0 = -\frac{T}{Z} \left(\frac{2E - U}{E - U} p_{-1}^0 + p_1^0 \right)$$

$$\left(E + \frac{T_{\mathbf{k}}^{\parallel}}{2} \frac{2E - U}{E - U} \right) p_{-1}^0 = -\frac{T}{2Z} \left(\frac{2E - U}{E - U} p_{-2}^0 + p_0^0 \right) \quad (\text{C5})$$

that yield the reflection amplitude R , Eq. 14 as well as the transmission amplitude \mathcal{T} , Eq. 15. Using Eq. (C4) we find the incoming, reflected and transmitted currents

$$\begin{aligned} j^{\text{in}} &= 2(2E - U)^2 \mathcal{N}^2 \sin(\kappa_{\text{Mott}}), \\ j^{\text{ref}} &= 2(2E - U)^2 \mathcal{N}^2 \sin(\kappa_{\text{Mott}}) |R|^2, \\ j^{\text{trans}} &= 2 \sin(\kappa_{\text{semi}}) |\mathcal{T}|^2. \end{aligned} \quad (\text{C6})$$

Hence, we find the transmission probability as the ratio of the two currents

$$\frac{j^{\text{trans}}}{j^{\text{in}}} = \frac{\sin(\kappa_{\text{Mott}}) \sin(\kappa_{\text{semi}})}{\sin\left(\frac{\kappa_{\text{Mott}} + \kappa_{\text{semi}}}{2}\right)^2} \quad (\text{C7})$$

This quickly drops to zero for $\kappa_{\text{Mott}} \neq \kappa_{\text{semi}}$, as shown in Fig. 1.

Appendix D: Tunneling through a Mott layer

Lastly, we want to look at the tunneling through a Mott layer sandwiched between two semiconductors. These semiconductors are both described by the same on-site potential V , but this can easily be generalized. The incoming spinor is given by

$$\begin{pmatrix} p_\mu^0 \\ p_\mu^1 \end{pmatrix} = \begin{pmatrix} x \\ 1 - x \end{pmatrix} (e^{i\kappa_{\text{semi}}\mu} + R e^{-i\kappa_{\text{semi}}\mu}), \quad (\text{D1})$$

the transmitted by

$$\begin{pmatrix} p_\mu^0 \\ p_\mu^1 \end{pmatrix} = \begin{pmatrix} x \\ 1 - x \end{pmatrix} T e^{i\kappa_{\text{semi}}\mu} \quad (\text{D2})$$

and inside the Mott insulator it takes the form

$$\begin{pmatrix} p_\mu^0 \\ p_\mu^1 \end{pmatrix} = \mathcal{N} \begin{pmatrix} E - U \\ E \end{pmatrix} (A e^{i\kappa\mu} + B e^{-i\kappa\mu}) \quad (\text{D3})$$

with the usual κ_{semi} and κ in the Mott insulator. As previously, $x = 0$ yields the valence band of the semiconductor, $x = 1$ the conduction band. The layer is supposed to have a thickness of d sites. Again, we deduct boundary conditions at the interfaces and find after some algebra the transmission

$$\frac{j_n^{\text{trans}}}{j_n^{\text{in}}} = \left| \frac{e^{id\kappa} e^{-i\kappa_{\text{semi}}d} (1 - e^{i2\kappa}) (1 - e^{i2\kappa_{\text{semi}}})}{(1 - e^{i\kappa} e^{i\kappa_{\text{semi}}})^2 - e^{i2d\kappa} (e^{i\kappa} - e^{i\kappa_{\text{semi}}})^2} \right|^2. \quad (\text{D4})$$

This is valid for transmitted and evanescent waves and shown in for transmission through the upper Hubbard band of the Mott insulator in Fig. 2. If both Mott bands do not match with the bands of the semiconductors, there are just decaying solutions $e^{-\kappa}$ with

$$\kappa = \text{arccosh} \left| \frac{Z}{2T} \left[\frac{E(U - E)}{E - U/2} - T_{\mathbf{k}}^{\parallel} \right] \right|. \quad (\text{D5})$$

There is still the possibility of tunneling. Now, for a number of layers $d \gg 1$ and $e^{-\kappa} < 1$ the transmission is given by

$$\frac{j_n^{\text{trans}}}{j_n^{\text{in}}} \approx 4e^{-2d\kappa} (1 - e^{-2\kappa})^2 (1 - \cos(\kappa_{\text{semi}}))^2. \quad (\text{D6})$$

For $E, T \ll U$ we find the tunneling solution as

$$e^{-\kappa} \approx \frac{4T(E - U/2)}{ZU^2}. \quad (\text{D7})$$

For an energy exactly between the two Hubbard bands $E = U/2$ the tunneling current vanishes identically. This was already predicted by the divergence of the Mott insulator dispersion relation in the main text.

Appendix E: Toy Model

In order to understand the strong suppression of tunneling through a Mott insulator in the middle between the upper and lower Hubbard band, i.e., for $E = U/2$, let us consider the following toy model consisting of three lattice sites in a row. The left and right lattice sites represent the semiconductor (where $V > 0$) and are tunnel coupled to the site in the middle which models the Mott insulator (with $U > 0$).

This scenario is very similar to a quantum dot in the Coulomb blockade regime tunnel coupled to two leads.

Now let us consider a second-order hopping process of a particle with spin \uparrow from the right to the left site. If the Mott site in the middle is also occupied by a particle with spin \uparrow , the only possible tunneling sequence is

$$|0\rangle |\uparrow\rangle |\uparrow\rangle \xrightarrow{T} |\uparrow\rangle |0\rangle |\uparrow\rangle \xrightarrow{T} |\uparrow\rangle |\uparrow\rangle |0\rangle, \quad (\text{E1})$$

which corresponds to the hole channel. The intermediate state $|\uparrow\rangle |0\rangle |\uparrow\rangle$ has an energy of $2V$ which is higher than the energy V of the initial and final states. Thus the amplitude of this second-order hopping process is $T^\uparrow = T^2/V$, see, e.g., [23].

On the other hand, if the Mott site in the middle is occupied by a particle with the other spin \downarrow , the only possible (second-order) tunneling sequence is

$$|0\rangle |\downarrow\rangle |\uparrow\rangle \xrightarrow{T} |0\rangle |\downarrow\rangle |0\rangle \xrightarrow{T} |\uparrow\rangle |\downarrow\rangle |0\rangle, \quad (\text{E2})$$

which corresponds to the particle channel.

Now the energy of the intermediate state $|0\rangle |\downarrow\rangle |0\rangle$ is given by U . As another difference, the \uparrow particle has to pass the \downarrow particle in the middle on its way, which results in a minus sign due to the fermionic nature of the creation and annihilation operators. Thus the amplitude for this second-order hopping process reads $T^\downarrow = -T^2/(U - V)$.

Comparing the two results, we see that the amplitudes have opposite signs, $T^\uparrow = -T^\downarrow$, in the middle between the upper and lower Hubbard band, i.e., for $V = U/2$.

If we now consider many of these rows in parallel, we may model the coherent propagation of a particle with transversal wavenumber \mathbf{k}^\parallel from right to left. Taking two rows and $\mathbf{k}^\parallel = 0$ for simplicity, the combination of the two results (E1) and (E2) yields

$$|0\rangle |\uparrow\rangle |\uparrow\rangle + |0\rangle |\uparrow\rangle |0\rangle \rightarrow T^\uparrow \begin{pmatrix} |\uparrow\rangle |\uparrow\rangle |0\rangle \\ |0\rangle |\downarrow\rangle |0\rangle \end{pmatrix} + T^\downarrow \begin{pmatrix} |0\rangle |\uparrow\rangle |0\rangle \\ |\uparrow\rangle |\downarrow\rangle |0\rangle \end{pmatrix}. \quad (\text{E3})$$

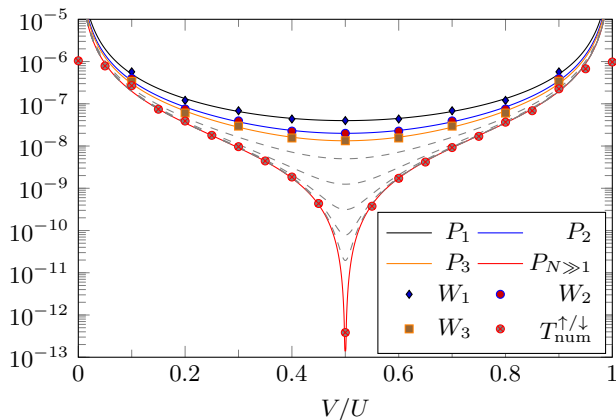


FIG. 3. (Color online) Transition probabilities P_N for coherent waves in the toy model for different numbers of rows N . The lines give the perturbation theory result, the black, blue and orange markers depict the properly rescaled numerical expectation values of the wave behind the Mott sites W_N . For $N = \infty$ the red circles give the probability using numerically obtained amplitudes T_\uparrow and T_\downarrow in Eq. (E6). The gray dashed lines give P_N for $N = 2^j$ with $j = 3, 5, 7, 9, 11$. The hopping strength is $T = 0.01 U$.

Due to the destructive interference between both channels, $T^\uparrow + T^\downarrow = 0$, the transition probability within the $\mathbf{k}^\parallel = 0$ sector vanishes. This is due to the Huygens mechanism, in which the coherent propagation of a particle can be understood via the constructive interference of the amplitudes from many lattice sites.

Note that the same destructive interference would occur if the spin in the Mott insulating site is oriented in x -direction $(|\uparrow\rangle + |\downarrow\rangle)/\sqrt{2}$, for example. Even if we consider one row only, the transport from right to left is only possible if that middle spin is flipped to $(|\uparrow\rangle - |\downarrow\rangle)/\sqrt{2}$, which also destroys the coherence of the propagation.

In the true Mott state, however, each of the middle sites must be modeled by the density matrix $\frac{1}{2}(|\uparrow\rangle\langle\uparrow| + |\downarrow\rangle\langle\downarrow|)$, see Eq. 3. Then, the cancellation in the transmission probability becomes first efficient at larger number of rows.

Since in this example the rows are not coupled with each other it is possible to obtain the transition probability for any number of rows N , including the limit of the infinite number of rows, analytically, based solely on the elementary amplitudes, T^\uparrow and T^\downarrow . The Mott insulating layer made up of N rows with N^\uparrow spin up and $N - N^\uparrow$ spin down electrons generates a tunnelling probability

$$P_{N^\uparrow} = \frac{|N^\uparrow T^\uparrow + (N - N^\uparrow) T^\downarrow|^2}{N^2}. \quad (\text{E4})$$

Summing up over all spins configurations, N^\uparrow , with the appropriate combinatorial factors yields the probability

$$P_N = \frac{N+1}{4N} (|T^\uparrow|^2 + |T^\downarrow|^2) + \frac{N-1}{2N} \text{Re}\{T^\uparrow T^{\downarrow*}\}. \quad (\text{E5})$$

This probability has a minimum for $T^\uparrow = -T^\downarrow$, which due to symmetry occurs in the middle of the gap for $V = U/2$, and falls as $1/N$. In the limit $N \gg 1$ we find

$$P_{N \gg 1} = \frac{1}{4} |T^\uparrow + T^\downarrow|^2 \quad (\text{E6})$$

which vanishes in the middle of the gap. This destructive interference is similar to the suppression of tunneling by a strong disorder potential. Using the perturbation theory amplitudes T^\uparrow, T^\downarrow given above we find for $N \gg 1$

$$P_{N \gg 1} = T^4 \frac{(V - \frac{U}{2})^2}{V^2(U - V)^2} \quad (\text{E7})$$

which is zero exactly at $V = U/2$.

The perturbative results have been compared with those obtained numerically. For a small number of rows N , the comparison of P_N is done with numerically obtained expectation values of the plane wave behind the Mott layers W_N . The initial state, composed of the Mott sites and the plane wave in the left semiconductor layer, is evolved forward in time and the expectation value of this wave behind the Mott region is measured. The W_N are rescaled in order to match the transmission probabilities at $V = U/2$ (since their normalization is unknown). For $N = 1, 2, 3$ Fig. 3 shows the P_N as functions of V/U (solid lines) together with the numerical results (markers with the same color). The numerical results agree very well with the perturbation theory (away of the poles at $V = 0$ and $V = U$): The $1/N$ behaviour in the middle of the gap and the shapes of the curves are confirmed. Furthermore, we calculated numerically the amplitudes T^\uparrow and T^\downarrow for a single row from the probabilities $|\langle \uparrow \uparrow | U(t) | 0 \uparrow \uparrow \rangle|^2$ and $|\langle \uparrow \downarrow | U(t) | 0 \uparrow \downarrow \rangle|^2$, respectively, using the full Hamiltonian. For short times, these probabilities grow quadratically in time with the prefactor equal to the second order hopping process [24]. By inserting them into Eq. (E6) we obtain the red squares in Fig. 3, which also agree very well with $P_{N \gg 1}$, including the drop in the transmission probability at $V = U/2$. The development of this suppression with growing N is indicated by the gray dashed lines.

[1] S. Pairault, D. Senechal, and A. Tremblay, Strong-coupling perturbation theory of the Hubbard model, The European Physical Journal B-Condensed Matter and

Complex Systems **16**, 85 (2000).

[2] M. Iskin and J. Freericks, Strong-coupling perturbation theory for the extended Bose-Hubbard model, Physical

- Review A **79**, 053634 (2009).
- [3] A. Georges, G. Kotliar, W. Krauth, and M. J. Rozenberg, Dynamical mean-field theory of strongly correlated fermion systems and the limit of infinite dimensions, *Reviews of Modern Physics* **68**, 13 (1996).
- [4] C. Kollath, A. M. Läuchli, and E. Altman, Quench dynamics and nonequilibrium phase diagram of the Bose-Hubbard model, *Physical Review Letters* **98**, 180601 (2007).
- [5] G. Biroli, C. Kollath, and A. M. Läuchli, Effect of rare fluctuations on the thermalization of isolated quantum systems, *Physical Review Letters* **105**, 250401 (2010).
- [6] G. Roux, Quenches in quantum many-body systems: One-dimensional Bose-Hubbard model reexamined, *Physical Review A* **79**, 021608 (2009).
- [7] M. Cramer, A. Flesch, I. P. McCulloch, U. Schollwöck, and J. Eisert, Exploring local quantum many-body relaxation by atoms in optical superlattices, *Physical Review Letters* **101**, 063001 (2008).
- [8] G. Stefanucci and S. Kurth, Steady-state density functional theory for finite bias conductances, *Nano Letters* **15**, 8020 (2015).
- [9] D. Jacob, G. Stefanucci, and S. Kurth, Mott Metal-transition from steady-state density functional theory, *Physical Review Letters* **125**, 216401 (2020).
- [10] V. Sunko, F. Mazzola, S. Kitamura, S. Khim, P. Kushwaha, O. J. Clark, M. D. Watson, I. Marković, D. Biswas, L. Pourovskii, T. K. Kim, T.-L. Lee, P. K. Thakur, H. Rosner, A. Georges, R. Moessner, T. Oka, A. P. Mackenzie, and P. D. C. King, Probing spin correlations using angle-resolved photoemission in a coupled metallic/Mott insulator system, *Science Advances* **6**, eaaz0611 (2020).
- [11] H.-J. Noh, J. Jeong, B. Chang, D. Jeong, H. S. Moon, E.-J. Cho, J. M. Ok, J. S. Kim, K. Kim, B. Min, *et al.*, Direct observation of localized spin antiferromagnetic transition in PdCrO₂ by angle-resolved photoemission spectroscopy, *Scientific reports* **4**, 1 (2014).
- [12] K. Yonemitsu, N. Maeshima, and T. Hasegawa, Suppression of rectification at metal-Mott insulator interfaces, *Physical Review B* **76**, 235118 (2007).
- [13] M. Jiang, G. Batrouni, and R. Scalettar, Density of states and magnetic correlations at a metal-Mott insulator interface, *Physical Review B* **86**, 195117 (2012).
- [14] E. Zhao, C. Zhang, and M. Lababidi, Mott scattering at the interface between a metal and a topological insulator, *Physical Review B* **82**, 205331 (2010).
- [15] R. Helmes, T. Costi, and A. Rosch, Kondo proximity effect: How does a metal penetrate into a Mott insulator?, *Physical Review Letters* **101**, 066802 (2008).
- [16] F. Queisser and R. Schützhold, Environment-induced prerelaxation in the Mott-Hubbard model, *Physical Review B* **99**, 155110 (2019).
- [17] F. Queisser, K. V. Krutitsky, P. Navez, and R. Schützhold, Equilibration and prethermalization in the Bose-Hubbard and Fermi-Hubbard models, *Physical Review A* **89**, 033616 (2014).
- [18] J. Hubbard, Electron correlations in narrow energy bands, *Proceedings of the Royal Society of London. Series A. Mathematical and Physical Sciences* **276**, 238 (1963).
- [19] I. Avigo, F. Queisser, P. Zhou, M. Ligges, K. Rossnagel, R. Schützhold, and U. Bovensiepen, Doublon bottleneck in the ultrafast relaxation dynamics of hot electrons in 1T-TaS₂, *Physical Review Research* **2**, 022046 (2020).
- [20] H. Im, Tunneling transport simulation in asymmetric junction devices with evanescent states at a junction interface, *Journal of the Korean Physical Society* **55**, 2512 (2009).
- [21] J. I. Choi, H. S. Kim, Y. S. Shin, C. Johnson, N. Fomina, P. Staley, C. Lang, and S. S. Jang, Electron-transport characteristics through aluminum oxide (100) and (012) in a metal-insulator-metal junction system: Density functional theory—nonequilibrium green function approach, *ACS Omega* **5**, 1717 (2020).
- [22] M. Koberidze, M. Puska, and R. Nieminen, Structural details of Al/Al₂O₃ junctions and their role in the formation of electron tunnel barriers, *Physical Review B* **97**, 195406 (2018).
- [23] J. Splettstoesser, M. Governale, and J. König, Tunneling-induced renormalization in interacting quantum dots, *Physical Review B* **86**, 035432 (2012).
- [24] N. Ahmadiyaz, M. Geller, J. König, P. Kratzer, A. Lorke, G. Schaller, and R. Schützhold, Quantum Zeno manipulation of quantum dots, *Phys. Rev. Res.* **4**, L032045 (2022).